*33rd EPS Conference on Plasma Phys. Rome, 19 - 23 June 2006 ECA Vol.**30I**, P-4.005 (2006)*

Traveling Wave Modes in a Helicon Plasma Source

John Rayner, Andrew Cheetham

University of Canberra, Canberra, Australia

1. Introduction: Helicon wave plasma sources have been studied for many years and are known to be useful for plasma processing applications [1, 2]. A feature of these sources is that they operate in a series of stable modes separated by non-linear jumps in plasma density that occur, for example, as the RF power coupled to the source increases. Several investigations have shown that one source of the jumps is the transition between different standing wave modes in the plasma set by the axial geometry of the source [3, 4, 5, 6]. Most of these studies, however, were for cylindrical plasma columns with fixed boundaries at each end leading to standing wave modes with nodes at each end and antinodes along the column.

In processing applications, the geometry often involves a helicon source, with one end closed, and the other coupled to a larger processing chamber. There is, therefore, the prospect of standing waves between the closed end and the antenna, and traveling waves propagating into the processing chamber. For efficient processing it would be desirable for as much of the radio frequency (RF) energy as possible to be carried by the traveling waves. This paper therefore aims to determine the conditions that optimise the production of traveling waves by adjusting the length of the cavity between the fixed end and the antenna for more efficient energy transfer into the traveling wave and hence the processing chamber.

2. The Experimental Arrangement: The helicon source consists of a 10 cm diameter Pyrex vacuum vessel with an effective working length ~100 cm, with an axial magnetic field from 0 to 600 G ±4%. One end of the vessel has a metal end plate located 54 cm from the antenna while the other end has a glass end cap 96 cm from the antenna. A stainless steel shaft that passes through the metal end plate carries a moveable stainless steel mesh baffle. The baffle can be moved axially thus providing effective cavity lengths L_0 in the range 15 cm < L_0 < 45 cm with respect to the antenna. The shaft also carries a Langmuir probe whose tip is located on the axis of the vessel and 10.0 cm in front of the baffle. The glass end cap on the other end of the vessel is far enough from the antenna for wave reflections not to occur. This configuration, with one end of the plasma vessel constrained while the other is essentially free approximates to a processing system in which the helicon source is placed next to a larger processing chamber. The plasma is excited by an m = 1 Boswell helicon antenna [1] with a length of 11 cm fed via a balanced transformer and matching network at 13.56 MHz by RF power up to 2.8 kW [7]. The working gas is Argon with pressures from 2 to 4 μbar.

The azimuthal component of the RF magnetic wave fields is monitored using *B*-dot coils mounted on the outside of the vessel.

3 Wavelength Measurements: Signals from the pick-up coils for the standing waves in the cavity were recorded using a digital oscilloscope together with signals for the traveling waves on the free side. The phase inversions of π for the standing waves and progressive phase shift for the traveling waves were clearly apparent. Wavelengths were obtained from these signals for a range of conditions. Since conditions were often unstable near to a jump an indirect means of determining the wavelength was employed using the dispersion relation for helicon waves [8, p437] and the expression for the saturation ion current for the Langmuir probe [8, p 174]. If these two expressions are combined then, for our probe, the wavelength λ (in cm), is related to the ion current I_i (in mA) by:

$$\lambda = \frac{5.87 \times 10^{-2} B_0 \beta \sqrt{T_e}}{I_i} \qquad [1]$$

where the electron temperature T_e is in eV, the axial magnetic field B_0 is in Gauss, and for the lowest order radial mode, $\beta = 3.1$.

Numerous measurements of wavelength for different values of the ion current showed that

$$\lambda I_i = C \qquad [2]$$

where C = 150±12 cm.mA is a constant compared with a theoretical value of 140 cm.mA based on equation (1) for our conditions (B_0 = 400 G, T_e = 3.5 eV). Wavelengths close to a jump could therefore be inferred based on the value of the ion current close to the jump.

4. Standing waves in the cavity: For a series of different cavity lengths, the wavelength of the standing wave was measured either directly from the pick-up coils or inferred from the ion current using equation [2] for a range of filling pressures and RF power levels. The measurements were made in three regimes: well below a jump, just below a jump and just above a jump.

Figure 1 plots the wavelength just below a jump as a function of cavity length L_0 for several pressures, plus the line $\lambda = 2L_0$ corresponding to a node under the antenna. The wavelengths cluster around this line and thus confirm that the jump occurs when an approximate node exists under the antenna. The scatter about this line may be attributed to the fact that the line represents the onset of an instability. We also found some evidence that the tuning of the matching network affects where the jump occurs.

Figure 2 plots the wavelengths just above the jump, and also those well below the jump, together with the lines for $\lambda=2L_0$ corresponding to a node under the antenna and $\lambda=4/3L_0$ and

λ=4L_0 corresponding to antinodes under the antenna. The results show that the stable mode below the jump corresponds to wavelengths in the range $2L_0<\lambda< 4L_0$ while above the jump $L_0<\lambda<4/3L_0$ thus confirming that stable modes occur when an approximate anti-node exists under the antenna.

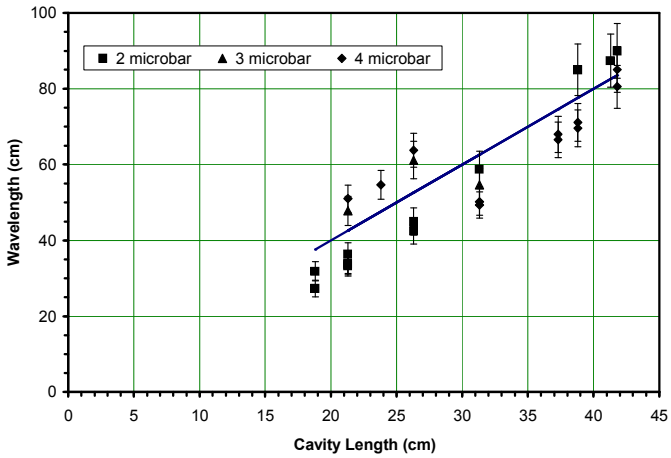

Figure 1: Wavelength just below the cavity mode jump as a function of cavity length. The line $\lambda = 2L_0$ for a node under the antenna is shown for comparison. *B* field: 400 G

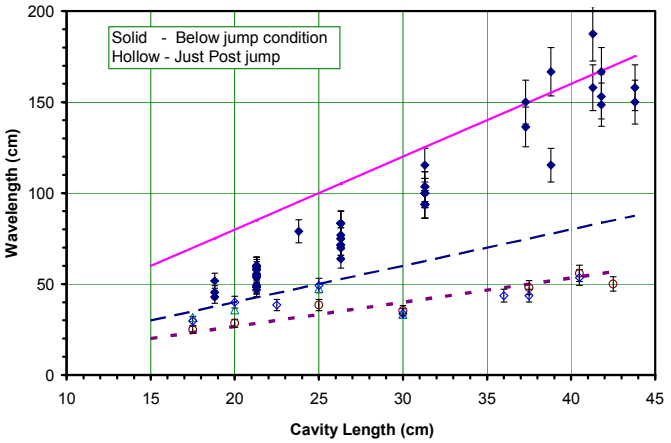

Figure 2: Wavelengths well below the jump (solid symbols) and also just above the jump (hollow symbols) as functions of cavity length. Also shown are the lines $\lambda = 2L_0$ (— —) for a node, and $\lambda = 4/3L_0$ (---) and $\lambda = 4L_0$ (—) for antinodes.

5. Traveling Waves Figure 3 shows the amplitudes of the traveling waves as a function of the ratio of the cavity length to wavelength. They have been normalised by dividing them by the power density to allow for different applied powers and cavity lengths. The results show a clear dip when the cavity is a half wavelength long leading to a node under the antenna, and so poor coupling of power into the waves.

The theoretical curve assumes that the applied power splits between the traveling and standing waves in the ratio of the impedances they present to the antenna. The cavity is modelled as a short-circuited lossy transmission line. For most lengths the cavity impedance is large compared with the traveling wave impedance. However if the length is ~ ½λ the impedance is small and so most of the power goes to the cavity. Large amplitude traveling waves therefore require the cavity to be ~ ¼λ, or ¾λ long.

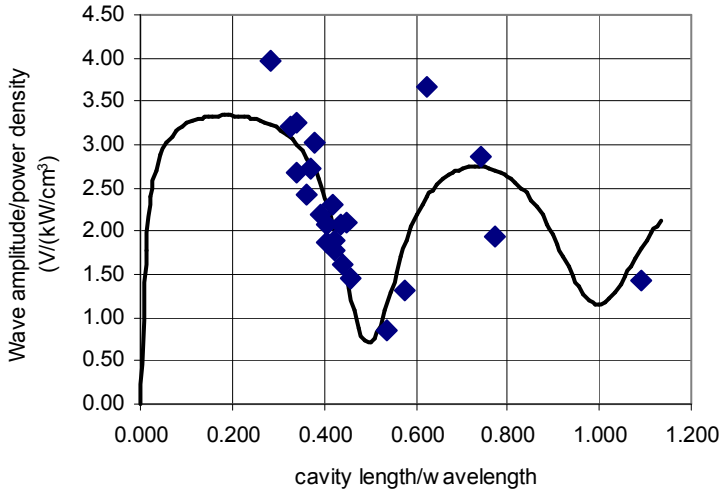

Figure 3: Traveling Wave Amplitudes as a function of cavity length/wavelength: experiment and theory.

6. Conclusions: We have observed both standing and traveling waves in a helicon plasma source with one fixed end and one free boundary. The simple helicon dispersion relation predicts to within ±8% the wavelength of both types of waves. We find that stable modes of operation exist when an approximate anti-node exists at the antenna. A node at the antenna results in poor coupling of the RF power and low amplitudes for the traveling waves. We support these results by a theoretical model in which we model the cavity as a short-circuited lossy transmission line and assume that the power splits in the ratio of the input impedance to the cavity and the intrinsic impedance of the traveling waves. Thus, for a helicon source used for processing applications the distance between the antenna and the end plate should produce an anti-node at the antenna as this not only leads to efficient coupling but also enhances the power transferred into the processing chamber by the traveling waves.

References.

1. Boswell R W 1984 *Plas. Phys. and Cont. Fusion* **26** 1147-1162.
2 Perry A J, Vender D and Boswell R W 1991 *J. Vac. Sci. Technol.* **B 9** 310-316
3. Kai C C, Sheridan T E and Boswell R W, 1999, *Plasma Sources Sci. Technol*, **8** 421-431
4. Lieberman M A and Boswell R W 1998 *J Phys IV France* **8** 145-164.
5. Nisoa M, Sakawa Y, and Shouji T 1999 *Jpn J. Appl. Phys*. **38** 777-779
6. Rayner J P and Cheetham A D 1999 *Plasma Sources Sci. Technol.* **8** 91-99.
7. Rayner J P, Cheetham A D and French G N 1996 *J. Vac. Sci. and Technol*. **A14** 2048-2055.
8. Lieberman M A and Lichtenberg A J 1994 *Principles of Plasma Discharges and Materials Processing* (J Wiley and Sons, New York).